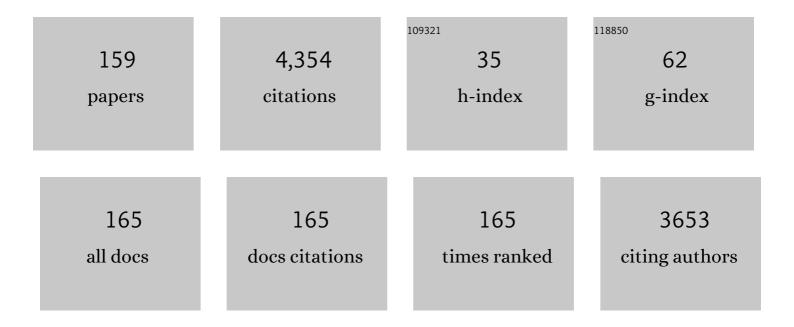
Antonio Pepe

List of Publications by Year in descending order

Source: https://exaly.com/author-pdf/6148884/publications.pdf Version: 2024-02-01



ANTONIO DEDE

#	Article	IF	CITATIONS
1	A Multigrid InSAR Technique for Joint Analyses at Single-Look and Multi-Look Scales. IEEE Geoscience and Remote Sensing Letters, 2022, 19, 1-5.	3.1	6
2	Atmospheric Phase Screen Compensation on Wrapped Ground-Based SAR Interferograms. IEEE Transactions on Geoscience and Remote Sensing, 2022, 60, 1-15.	6.3	8
3	Changes of Chinese Coastal Regions Induced by Land Reclamation as Revealed through TanDEM-X DEM and InSAR Analyses. Remote Sensing, 2022, 14, 637.	4.0	6
4	Near Real-Time InSAR Deformation Time Series Estimation With Modified Kalman Filter and Sequential Least Squares. IEEE Journal of Selected Topics in Applied Earth Observations and Remote Sensing, 2022, 15, 2437-2448.	4.9	5
5	On the Exploitation of Remote Sensing Technologies for the Monitoring of Coastal and River Delta Regions. Remote Sensing, 2022, 14, 2384.	4.0	6
6	Change Detection Techniques with Synthetic Aperture Radar Images: Experiments with Random Forests and Sentinel-1 Observations. Remote Sensing, 2022, 14, 3323.	4.0	24
7	Multi-Temporal Small Baseline Interferometric SAR Algorithms: Error Budget and Theoretical Performance. Remote Sensing, 2021, 13, 557.	4.0	13
8	Analysis of Groundwater Depletion/Inflation and Freeze–Thaw Cycles in the Northern Urumqi Region with the SBAS Technique and an Adjusted Network of Interferograms. Remote Sensing, 2021, 13, 2144.	4.0	5
9	Recent advancements in multi-temporal methods applied to new generation SAR systems and applications in South America. Journal of South American Earth Sciences, 2021, 111, 103410.	1.4	10
10	Structural Controls Over the 2019 Ridgecrest Earthquake Sequence Investigated by Highâ€Fidelity Elastic Models of 3D Velocity Structures. Journal of Geophysical Research: Solid Earth, 2021, 126, e2020JB021124.	3.4	5
11	Integrated Analysis of the Combined Risk of Ground Subsidence, Sea Level Rise, and Natural Hazards in Coastal and Delta River Regions. Remote Sensing, 2021, 13, 3431.	4.0	5
12	Adaptive Multilooking of Multitemporal Differential SAR Interferometric Data Stack Using Directional Statistics. IEEE Transactions on Geoscience and Remote Sensing, 2021, 59, 6706-6721.	6.3	10
13	Long-Term Continuously Updated Deformation Time Series From Multisensor InSAR in Xi'an, China From 2007 to 2021. IEEE Journal of Selected Topics in Applied Earth Observations and Remote Sensing, 2021, 14, 7297-7309.	4.9	12
14	Tropospheric Excess Path Delay Compensation on Wrapped Ground-Based SAR Interferograms. , 2021, , .		0
15	The Triplet Network Enhanced Spectral Diversity (T-NESD) Method for the Correction of TOPS Data Co-registration Errors for Non-Stationary Scenes. , 2021, , .		1
16	High Performance Computing in Satellite SAR Interferometry: A Critical Perspective. Remote Sensing, 2021, 13, 4756.	4.0	10
17	On the Characterization and Forecasting of Ground Displacements of Ocean-Reclaimed Lands. Remote Sensing, 2020, 12, 2971.	4.0	8
18	On the Use of Weighted Least-Squares Approaches for Differential Interferometric SAR Analyses: The Weighted Adaptive Variable-IEngth (WAVE) Technique. Sensors, 2020, 20, 1103.	3.8	10

ΑΝΤΟΝΙΟ ΡΕΡΕ

#	Article	IF	CITATIONS
19	Investigation of the ground displacement in Saint Petersburg, Russia, using multiple-track differential synthetic aperture radar interferometry. International Journal of Applied Earth Observation and Geoinformation, 2020, 87, 102050.	2.8	8
20	The Multiple Aperture SAR Interferometry (MAI) Technique for the Detection of Large Ground Displacement Dynamics: An Overview. Remote Sensing, 2020, 12, 1189.	4.0	27
21	An Adaptive Statistical Multi-grid DInSAR Technique for Studying Multi-scale Earth Surface Deformation Phenomena. , 2020, , .		1
22	A Generalized-SVD-Based Technique for Enhancing Performance of Multi-Temporal Dinsar Analyses: The Weighted Adaptive Variable-Length (Wave) Technique. , 2020, , .		0
23	The Correction of Phase Unwrapping Errors in Sequences of Multi-Temporal Differential SAR Interferograms. , 2020, , .		2
24	A Phase-Preserving Focusing Technique for TOPS Mode SAR Raw Data Based on Conventional Processing Methods. Sensors, 2019, 19, 3321.	3.8	4
25	Volcanic structures investigation through SAR and seismic interferometric methods: The 2011–2013 Campi Flegrei unrest episode. Remote Sensing of Environment, 2019, 234, 111440.	11.0	22
26	Generation of long-term InSAR ground displacement time-series through a novel multi-sensor data merging technique: The case study of the Shanghai coastal area. ISPRS Journal of Photogrammetry and Remote Sensing, 2019, 154, 10-27.	11.1	40
27	The Parallel SBAS Approach for Sentinel-1 Interferometric Wide Swath Deformation Time-Series Generation: Algorithm Description and Products Quality Assessment. IEEE Transactions on Geoscience and Remote Sensing, 2019, 57, 6259-6281.	6.3	119
28	DInSAR Analysis and Analytical Modeling of Mount Etna Displacements: The December 2018 Volcanoâ€Tectonic Crisis. Geophysical Research Letters, 2019, 46, 5817-5827.	4.0	73
29	Theory and Statistical Description of the Enhanced Multi-Temporal InSAR (E-MTInSAR) Noise-Filtering Algorithm. Remote Sensing, 2019, 11, 363.	4.0	13
30	Long-term flood-hazard modeling for coastal areas using InSAR measurements and a hydrodynamic model: The case study of Lingang New City, Shanghai. Journal of Hydrology, 2019, 571, 593-604.	5.4	26
31	The Deforming Etna Volcano Imaged Through SBAS-DInSAR Analysis: its Long Term Behaviour and the Recent Seismo-Volcanic Crisis of December 2018. , 2019, , .		0
32	Monitoring Volcano Deformation from Space with Sentinel-1 Data for Civil Protection. , 2019, , .		1
33	Coseismic Stress and Strain Field Changes Investigation Through 3â€Ð Finite Element Modeling of DInSAR and GPS Measurements and Geological/Seismological Data: The L'Aquila (Italy) 2009 Earthquake Case Study. Journal of Geophysical Research: Solid Earth, 2018, 123, 4193-4222.	3.4	20
34	Hybrid Stripmap–ScanSAR Interferometry: Extension to the X-Band COSMO-SkyMed Data. IEEE Geoscience and Remote Sensing Letters, 2018, 15, 330-334.	3.1	3
35	The 21 August 2017 Ischia (Italy) Earthquake Source Model Inferred From Seismological, GPS, and DInSAR Measurements. Geophysical Research Letters, 2018, 45, 2193-2202.	4.0	59
36	Gical: Geo-Morphometric Inverse Cylindrical Method for Radiometric Calibration of Sar Images. , 2018,		3

3

,.

Αντόνιο Ρερε

#	Article	IF	CITATIONS
37	Polarimetric Sar Distortions Induced by Topography: an Analytical Formulation for Compensation in the Imaging Domain. , 2018, , .		2
38	Exploitation of Copernicus Sentinels Data for Sensing Fire-Disturbed Vegetated Areas. , 2018, , .		5
39	The Parallel SBAS-Dinsar Processing Chain for Massive Generation of Sentinel-1 Deformation Time-Series. , 2018, , .		0
40	Surface Deformation of the Shanghai Coastal Area Revealed by a Multi-Satellite Dinsar Investigation. , 2018, , .		0
41	The "Urban Geomatics for Bulk Information Generation, Data Assessment and Technology Awareness― Project: Detection, Representation and Analysis of the Urban Scenario Changes. , 2018, , .		2
42	Potential and Limitations of Open Satellite Data for Flood Mapping. Remote Sensing, 2018, 10, 1673.	4.0	105
43	Low cost, multiscale and multi-sensor application for flooded area mapping. Natural Hazards and Earth System Sciences, 2018, 18, 1493-1516.	3.6	39
44	Comparative study of SAR interferometric phase filtering algoithms. , 2018, , .		3
45	Finite element modelling of the 2015 Gorkha earthquake through the joint exploitation of DInSAR measurements and geologic-structural information. Tectonophysics, 2017, 714-715, 125-132.	2.2	12
46	Source modelling of the 2015 Wolf volcano (Galápagos) eruption inferred from Sentinel 1-A DInSAR deformation maps and pre-eruptive ENVISAT time series. Journal of Volcanology and Geothermal Research, 2017, 344, 246-256.	2.1	19
47	Aftershocks, groundwater changes and postseismic ground displacements related to pore pressure gradients: Insights from the 2012 Emiliaâ€Romagna earthquake. Journal of Geophysical Research: Solid Earth, 2017, 122, 5622-5638.	3.4	18
48	The role of thermo-rheological properties of the crust beneath Ischia Island (Southern Italy) in the modulation of the ground deformation pattern. Journal of Volcanology and Geothermal Research, 2017, 344, 154-173.	2.1	27
49	Geodetic model of the 2016 Central Italy earthquake sequence inferred from InSAR and GPS data. Geophysical Research Letters, 2017, 44, 6778-6787.	4.0	162
50	Effect of the Vegetation Fire on Backscattering: An Investigation Based on Sentinel-1 Observations. IEEE Journal of Selected Topics in Applied Earth Observations and Remote Sensing, 2017, 10, 4478-4492.	4.9	51
51	Volcano Geodesy: Recent developments and future challenges. Journal of Volcanology and Geothermal Research, 2017, 344, 1-12.	2.1	61
52	New insights on the 2012–2013 uplift episode at Fernandina Volcano (Galápagos). Geophysical Journal International, 2017, 211, 673-685.	2.4	7
53	Sentinel-1 TOPS data focusing based on a modified two-step processing approach. , 2017, , .		1
54	DEM correction and mean surface displacement rate retrieval from a stack of wrapped multi-temporal DInSAR interferograms. , 2017, , .		0

ΑΝΤΟΝΙΟ ΡΕΡΕ

#	Article	IF	CITATIONS
55	Sentinel-1 data exploitation for automatic surface deformation time-series generation through the SBAS-DInSAR parallel processing chain. , 2017, , .		Ο
56	DInSAR-Based Detection of Land Subsidence and Correlation with Groundwater Depletion in Konya Plain, Turkey. Remote Sensing, 2017, 9, 83.	4.0	59
57	The 2015–2016 Ground Displacements of the Shanghai Coastal Area Inferred from a Combined COSMO-SkyMed/Sentinel-1 DInSAR Analysis. Remote Sensing, 2017, 9, 1194.	4.0	28
58	On the use of directional statistics for the adaptive spatial multi-looking of sequences of differential SAR interferograms. , 2017, , .		1
59	A Review of Interferometric Synthetic Aperture RADAR (InSAR) Multi-Track Approaches for the Retrieval of Earth's Surface Displacements. Applied Sciences (Switzerland), 2017, 7, 1264.	2.5	199
60	Potential inundated coastal area estimation in Shanghai with multi-platform SAR and altimetry data. , 2017, , .		1
61	Residual settlements detection of ocean reclaimed lands with multi-platform SAR time series and SBAS technique: a case study of Shanghai Pudong International Airport. , 2017, , .		1
62	Topological Characterization and Advanced Noise-Filtering Techniques for Phase Unwrapping of Interferometric Data Stacks. , 2016, , .		2
63	The Use of C-/X-Band Time-Gapped SAR Data and Geotechnical Models for the Study of Shanghai's Ocean-Reclaimed Lands through the SBAS-DInSAR Technique. Remote Sensing, 2016, 8, 911.	4.0	63
64	Ground deformation and source geometry of the 24 August 2016 Amatrice earthquake (Central Italy) investigated through analytical and numerical modeling of DInSAR measurements and structuralâ€geological data. Geophysical Research Letters, 2016, 43, 12,389.	4.0	124
65	Evidence of a shallow persistent magmatic reservoir from joint inversion of gravity and ground deformation data: The 25–26 October 2013 Etna lava fountaining event. Geophysical Research Letters, 2016, 43, 3246-3253.	4.0	13
66	Unsupervised parallel SBAS-DInSAR chain for massive and systematic Sentinel-1 data processing. , 2016, , \cdot		7
67	A Minimum Acceleration Approach for the Retrieval of Multiplatform InSAR Deformation Time Series. IEEE Journal of Selected Topics in Applied Earth Observations and Remote Sensing, 2016, 9, 3883-3898.	4.9	52
68	Automatic and Systematic Sentinel-1 SBAS-DInSAR Processing Chain for Deformation Time-series Generation. Procedia Computer Science, 2016, 100, 1176-1180.	2.0	14
69	Spaceborne Synthetic Aperture Radar Data Focusing on Multicore-Based Architectures. IEEE Transactions on Geoscience and Remote Sensing, 2016, 54, 4712-4731.	6.3	17
70	Sentinel-1 results: SBAS-DInSAR processing chain developments and land subsidence analysis. , 2015, , .		8
71	Remote sensing of burned area: A fuzzy-based framework for joint processing of optical and microwave data. , 2015, , .		2
72	Integration of Optical and SAR Data for Burned Area Mapping in Mediterranean Regions. Remote Sensing, 2015, 7, 1320-1345.	4.0	69

Αντόνιο Ρερε

#	Article	IF	CITATIONS
73	The Space-Borne SBAS-DInSAR Technique as a Supporting Tool for Sustainable Urban Policies: The Case of Istanbul Megacity, Turkey. Remote Sensing, 2015, 7, 16519-16536.	4.0	27
74	Improved EMCF-SBAS Processing Chain Based on Advanced Techniques for the Noise-Filtering and Selection of Small Baseline Multi-Look DInSAR Interferograms. IEEE Transactions on Geoscience and Remote Sensing, 2015, 53, 4394-4417.	6.3	92
75	Recent advancements of the Stripmap-ScanSAR differential SAR interferometry using X-band COSMO-SkyMed data. , 2015, , .		Ο
76	The study of the deformation time evolution in coastal areas of Shanghai: A joint C/X-band SBAS-DINSAR analysis. , 2015, , .		3
77	Accurate DInSAR stack coherence estimation exploiting phase statistics. , 2015, , .		0
78	A segmented block processing approach to focus synthetic aperture radar data on multicore processors. , 2015, , .		1
79	High-performance parallel computation of the multichannel phase unwrapping problem. , 2015, , .		2
80	Multichannel Phase Unwrapping: Problem Topology and Dual-Level Parallel Computational Model. IEEE Transactions on Geoscience and Remote Sensing, 2015, 53, 5774-5793.	6.3	14
81	The Constrained-Network Propagation (C-NetP) Technique to Improve SBAS-DInSAR Deformation Time Series Retrieval. IEEE Journal of Selected Topics in Applied Earth Observations and Remote Sensing, 2015, 8, 4910-4921.	4.9	12
82	Magma and fluid migration at Yellowstone Caldera in the last three decades inferred from InSAR, leveling, and gravity measurements. Journal of Geophysical Research: Solid Earth, 2015, 120, 2627-2647.	3.4	42
83	A DInSAR Investigation of the Ground Settlement Time Evolution of Ocean-Reclaimed Lands in Shanghai. IEEE Journal of Selected Topics in Applied Earth Observations and Remote Sensing, 2015, 8, 1763-1781.	4.9	48
84	Quantifying the effects of ground settlement on buildings by the exploitation of long term DINSAR time series: The case of Roma. , 2015, , .		3
85	A Parallel Computational Model for Multichannel Phase Unwrapping Problem. , 2015, , .		0
86	Processing Optical and SAR data for burned forests mapping: An integrated framework. , 2015, , .		0
87	A Minimum Curvature Combination Method for the Generation of Multi-platform DInSAR Deformation Time-Series. , 2015, , .		4
88	A differential SAR interferometry (DInSAR) investigation of the deformation affecting the coastal reclaimed areas of the Shangai megacity. , 2014, , .		2
89	Possible coupling of Campi Flegrei and Vesuvius as revealed by InSAR time series, correlation analysis and time dependent modeling. Journal of Volcanology and Geothermal Research, 2014, 280, 104-110.	2.1	17
90	How second generation SAR systems are impacting the analysis of ground deformation. International Journal of Applied Earth Observation and Geoinformation, 2014, 28, 1-11.	2.8	55

ANTONIO PEPE

#	Article	IF	CITATIONS
91	From Previous C-Band to New X-Band SAR Systems: Assessment of the DInSAR Mapping Improvement for Deformation Time-Series Retrieval in Urban Areas. IEEE Transactions on Geoscience and Remote Sensing, 2013, 51, 1973-1984.	6.3	79
92	A full exploitation of the enhanced SBAS-DInSAR approach in volcanic and seismogenic areas. , 2013, , .		1
93	Analysis of the SBAS-DInSAR displacement time-series accuracies retrieved in volcanic areas through the first and second generation sensor SAR data. , 2013, , .		2
94	New insights into the 2012 Emilia (Italy) seismic sequence through advanced numerical modeling of ground deformation InSAR measurements. Geophysical Research Letters, 2013, 40, 1971-1977.	4.0	53
95	Time series of SAR image fractal maps. , 2013, , .		0
96	A simple solution to mitigate noise effects in time-redundant sequences of small baseline multi-look DInSAR interferograms. Remote Sensing Letters, 2013, 4, 609-618.	1.4	26
97	Ground deformation associated with the 2012 Emilia (Northern Italy) seismic crisis retrieved through spaceborne SAR interferometry. , 2013, , .		0
98	A region-growing technique to improve multi-temporal DInSAR interferogram phase unwrapping performance. Remote Sensing Letters, 2013, 4, 988-997.	1.4	15
99	Seismoâ€ŧectonic behavior of the Pernicana Fault System (Mt Etna): A gauge for volcano flank instability?. Journal of Geophysical Research: Solid Earth, 2013, 118, 4398-4409.	3.4	29
100	Capturing the fingerprint of Etna volcano activity in gravity and satellite radar data. Scientific Reports, 2013, 3, 3089.	3.3	20
101	An innovative region growing algorithm based on Minimum Cost Flow approach for Phase Unwrapping of full-resolution differential interferograms. , 2012, , .		8
102	Cosmo-SkyMed AO projects - exploitation of fractal scattering models for Cosmo-SkyMed images interpretation. , 2012, , .		0
103	DInSAR deformation time series for monitoring urban areas: The impact of the second generation SAR systems. , 2012, , .		0
104	A new SBAS-DInSAR approach based on a redundant set of small baseline interferograms. , 2012, , .		2
105	Long term deformation time series: 10 years of Earth observation through ENVISAT multi-mode ASAR sensor. , 2012, , .		0
106	Analysis of ground deformation using SBAS-DInSAR technique applied to COSMO-SkyMed images, the test case of Roma urban area. Proceedings of SPIE, 2012, , .	0.8	7
107	Integration of optical and SAR remotely sensed data for monitoring wildfires in Mediterranean forests. , 2012, , .		2
108	A quantitative assessment of DInSAR Time series accuracy in volcanic areas: From the first to second generation SAR sensors. , 2012, , .		0

ANTONIO PEPE

#	Article	IF	CITATIONS
109	Modeling of ALOS and COSMO-SkyMed satellite data at Mt Etna: Implications on relation between seismic activation of the Pernicana fault system and volcanic unrest. Remote Sensing of Environment, 2012, 125, 64-72.	11.0	17
110	A Quantitative Assessment of DInSAR Measurements of Interseismic Deformation: The Southern San Andreas Fault Case Study. Pure and Applied Geophysics, 2012, 169, 1463-1482.	1.9	97
111	The Stripmap–ScanSAR SBAS Approach to Fill Gaps in Stripmap Deformation Time Series With ScanSAR Data. IEEE Transactions on Geoscience and Remote Sensing, 2011, 49, 4788-4804.	6.3	29
112	New Advances of the Extended Minimum Cost Flow Phase Unwrapping Algorithm for SBAS-DInSAR Analysis at Full Spatial Resolution. IEEE Transactions on Geoscience and Remote Sensing, 2011, 49, 4062-4079.	6.3	40
113	SBAS-Based Satellite Orbit Correction for the Generation of DInSAR Time-Series: Application to RADARSAT-1 Data. IEEE Transactions on Geoscience and Remote Sensing, 2011, 49, 5150-5165.	6.3	53
114	Long-term deformation analysis of historical buildings through the advanced SBAS-DInSAR technique: the case study of the city of Rome, Italy. Journal of Geophysics and Engineering, 2011, 8, S1-S12.	1.4	44
115	On the Generation of Late ERS Deformation Time Series Through Small Doppler and Baseline Subsets Differential SAR Interferograms. IEEE Geoscience and Remote Sensing Letters, 2011, 8, 238-242.	3.1	4
116	Deformation Time-Series Generation in Areas Characterized by Large Displacement Dynamics: The SAR Amplitude Pixel-Offset SBAS Technique. IEEE Transactions on Geoscience and Remote Sensing, 2011, 49, 2752-2763.	6.3	148
117	New improvements of the extended minimum cost flow phase unwrapping for processing multitemporal full resolution interferograms. , 2011, , .		1
118	SBAS-DInSAR time series in the last eighteen years at Mt. Etna volcano (Italy). , 2011, , .		2
119	Analysis of the 1992–2010 dynamic deformation affecting the Yellowstone Caldera. , 2011, , .		0
120	Deformation in Hawaii's volcanoes obtained from a ScanSAR-to-stripmap Small BAseline Subset technique. , 2010, , .		0
121	Full exploitation of the SBAS-DInSAR algorithm in active seismogenetic scenarios. , 2010, , .		0
122	Advances in the generation of deformation time series from SAR data sequences in areas affected by large dynamics. , 2010, , .		0
123	Detachment depth revealed by rollover deformation: An integrated approach at Mount Etna. Geophysical Research Letters, 2010, 37, .	4.0	37
124	Surface displacements associated with the L'Aquila 2009 Mw 6.3 earthquake (central Italy): New evidence from SBASâ€ÐInSAR time series analysis. Geophysical Research Letters, 2010, 37, .	4.0	84
125	Longâ€ŧerm versus shortâ€ŧerm deformation processes at Tenerife (Canary Islands). Journal of Geophysical Research, 2010, 115, .	3.3	11
126	RADARSAT-1 deformation time-series generation by using the SBAS-DInSAR algorithm. , 2009, , .		0

ΑΝΤΟΝΙΟ ΡΕΡΕ

#	Article	IF	CITATIONS
127	Analysis of Ground Deformation Detected Using the SBAS-DInSAR Technique in Umbria, Central Italy. Pure and Applied Geophysics, 2009, 166, 1425-1459.	1.9	83
128	Surface deformation in the Abruzzi region, Central Italy, from multitemporal DInSAR analysis. Geophysical Journal International, 2009, 178, 1193-1197.	2.4	20
129	Gravityâ€driven deformation of Tenerife measured by InSAR time series analysis. Geophysical Research Letters, 2009, 36, .	4.0	47
130	Stress transfer in the Lazufre volcanic area, central Andes. Geophysical Research Letters, 2009, 36, .	4.0	36
131	RADARSAT-1 deformation time-series analysis based on the SBAS-DInSAR algorithm. , 2009, , .		1
132	Analysis of Ground Deformation Detected Using the SBAS-DInSAR Technique in Umbria, Central Italy. , 2009, , 1425-1459.		3
133	Surface deformation of active volcanic areas retrieved with the SBAS-DInSAR technique: an overview. Annals of Geophysics, 2009, 51, .	1.0	2
134	On the fractal dimension of the fallout deposits: A case study of the 79ÂA.D. Plinian eruption at Mt. Vesuvius. Journal of Volcanology and Geothermal Research, 2008, 177, 288-299.	2.1	9
135	The 2004–2006 uplift episode at Campi Flegrei caldera (Italy): Constraints from SBASâ€ÐInSAR ENVISAT data and Bayesian source inference. Geophysical Research Letters, 2008, 35, .	4.0	66
136	SBAS-DInSAR Analysis of Very Extended Areas: First Results on a 60 000-\$hbox{km}^{2}\$ Test Site. IEEE Geoscience and Remote Sensing Letters, 2008, 5, 438-442.	3.1	32
137	Surface deformation analysis of the Campi Flegrei caldera, Italy, by exploiting the ENVISAT ASAR data with the SBAS-DInSAR technique. , 2007, , .		0
138	The SBAS-DInSAR technique as a tool for the observation of active volcanic areas: Results and future perspectives. , 2007, , .		1
139	A space-time minimum cost flow phase unwrapping algorithm for the generation of persistent scatterers deformation time-series. , 2007, , .		5
140	An Overview of the Small BAseline Subset Algorithm: A DInSAR Technique for Surface Deformation Analysis. , 2007, , 637-661.		34
141	An Overview of the Small BAseline Subset Algorithm: a DInSAR Technique for Surface Deformation Analysis. Pure and Applied Geophysics, 2007, 164, 637-661.	1.9	295
142	Analysis of seven maternal polymorphisms of genes involved in homocysteine/folate metabolism and risk of Down syndrome offspring. Genetics in Medicine, 2006, 8, 409-416.	2.4	109
143	Joint analysis of SAR interferometry and electrical resistivity tomography surveys for investigating ground deformation: the case-study of Satriano di Lucania (Potenza, Italy). Engineering Geology, 2006, 88, 260-273.	6.3	31
144	On the Extension of the Minimum Cost Flow Algorithm for Phase Unwrapping of Multitemporal Differential SAR Interferograms. IEEE Transactions on Geoscience and Remote Sensing, 2006, 44, 2374-2383.	6.3	309

ANTONIO PEPE

#	Article	IF	CITATIONS
145	On the Generation of ERS/ENVISAT DInSAR Time-Series Via the SBAS Technique. IEEE Geoscience and Remote Sensing Letters, 2005, 2, 265-269.	3.1	99
146	Volcanic spreading of Vesuvius, a new paradigm for interpreting its volcanic activity. Geophysical Research Letters, 2005, 32, .	4.0	86
147	Gravity and magma induced spreading of Mount Etna volcano revealed by satellite radar interferometry. Geophysical Research Letters, 2004, 31, .	4.0	165
148	A differential SAR interferometry approach for monitoring urban deformation phenomena. , 2003, , .		6
149	MINERVA: an INSAR monitoring system for volcanic hazard. , 0, , .		0
150	A two-scale differential SAR interferometry approach for investigating earth surface deformations. , 0, , .		5
151	Large scale InSAR deformation time series: Phoenix and Houston case studies. , 0, , .		5
152	A space-time minimum cost flow phase unwrapping algorithm for the generation of DInSAR deformation time-series. , 0, , .		1
153	Satellite SAR Interferometry for Earth's Crust Deformation Monitoring and Geological Phenomena Analysis. , 0, , .		2
154	Generation of Earth's Surface Three-Dimensional (3-D) Displacement Time-Series by Multiple-Platform SAR Data. , 0, , .		1
155	A MULTI-SOURCE DATA APPROACH FOR THE INVESTIGATION OF LAND SUBSIDENCE IN THE KONYA BASIN, TURKEY. International Archives of the Photogrammetry, Remote Sensing and Spatial Information Sciences - ISPRS Archives, 0, XLII-3/W4, 129-135.	0.2	10
156	VISUALIZATION OF BIG GEODATA: AN EXPERIMENT WITH DINSAR DEFORMATION TIME SERIES. International Archives of the Photogrammetry, Remote Sensing and Spatial Information Sciences - ISPRS Archives, 0, XLII-4/W14, 135-141.	0.2	1
157	Analysis of deformation patterns through advanced DINSAR techniques in Istanbul megacity. International Archives of the Photogrammetry, Remote Sensing and Spatial Information Sciences - ISPRS Archives, 0, XL-7, 19-21.	0.2	0
158	URBAN GEO BIG DATA. International Archives of the Photogrammetry, Remote Sensing and Spatial Information Sciences - ISPRS Archives, 0, XLII-4/W14, 23-30.	0.2	4
159	EVALUATION OF DEM DERIVED BY REPEAT-PASS X-BAND STRIPMAP MODE PAZ DATA. International Archives of the Photogrammetry, Remote Sensing and Spatial Information Sciences - ISPRS Archives, 0, XLIII-B3-2022, 243-248.	0.2	Ο